2003

Comparison between hydrogen and dihydrogen bonds among H3BNH3, H2BNH2, and NH3

T. Kar

Steve Scheiner
Utah State University

Recommended Citation
Comparison between hydrogen and dihydrogen bonds among H[sub 3]BNH[sub 3], H[sub 2]BNH[sub 2], and NH[sub 3] Tapas Kar and Steve Scheiner, J. Chem. Phys. 119, 1473 (2003), DOI:10.1063/1.1580093

Comparison between hydrogen and dihydrogen bonds among H_3BNH_3, H_2BNH_2, and NH_3

Tapas Kar[a] and Steve Scheiner
Department of Chemistry and Biochemistry, Utah State University, Logan, Utah 84322-0300

(Received 5 March 2003; accepted 15 April 2003)

Several possible binary complexes among ammonia-borane, aminoborane, and ammonia, via hydrogen and/or dihydrogen bonds, have been investigated to understand the effect of different hybridization. Møller–Plesset second-order perturbation theory with aug-cc-pVDZ basis set was used. The interaction energy is corrected for basis set superposition error, and the Morokuma–Kitaura method was employed to decompose the total interaction energy. Like H_3BNH_3, the sp^2 hybridized H_2BNH_2 also participates in H- and dihydrogen bond formation. However, such bonds are weaker than their sp^3 analogs. The contractions of BN bonds are associated with blueshift in vibrational frequency and stretches of BH and NH bonds with redshift. The polarization, charge transfer, correlation, and higher-order energy components are larger in dihydrogen bonded complexes, compared to classical H-bonded ammonia dimers. © *2003 American Institute of Physics.* [DOI: 10.1063/1.1580093]

INTRODUCTION

The study of hydrogen bonding has been an active field of research for several decades,[1–4] and its role is well established in the stabilization of biological macromolecules, enhancing the selective binding of substrates to their enzymes, base pairing in nucleic acids, and as a precursor to proton transfer reactions. H bonds are represented by the notation $X–H\cdots Y$, where X and Y refer to conventional proton donors (such as O–H or N–H) and acceptors (a lone pair of electrons of an electronegative element, such as O, N, or halogens), respectively. Hydrogen bonds that make use of other than these donors and/or acceptors are commonly termed unconventional H bonds. Different types of unconventional hydrogen bonds have been reported[5] during the last decade. For example, π-hydrogen bonds[6–10] (where the acceptors correspond to π electron density) and $C–H\cdots O/N$ bonds[11–13] (where the donors are C–H) have been described. We have recently reported[14] a comparative study of these three sorts of H bonds involving aromatic amino acids and H_2O.

In all these $X–H\cdots Y$ H bonds, the bridging hydrogen atoms lose electron density while X (C, O, N, etc.) and Y (O, N, halogens, and π systems) atoms gain. The literature also contains references to a completely different type of hydrogen bond, where the bridging hydrogen atom gains electrons and other nonhydrogen atoms accept them. For example, $X–H^{\delta-}\cdots Y$ is such a bond where X and Y represent electron deficient or electropositive atoms, such as LiH, BeH_2, and BH_4^-. This type of hydrogen bond is termed ''inverse'' H bonds.[15] Such a bond, involving bridging lithium atom (such as $Li–H\cdots Li–H$) as in linear $(LiH)_2$, is also known as an Li bond.[16]

Another class of unconventional H bonds where both kinds of hydrogen atoms ($H^{\delta-}$ and $H^{\delta+}$) are present are known as dihydrogen bonds (DHB).[17] They are represented by the notation $M–H\cdots H–Y$, where M refers to an element less electronegative than hydrogen and Y to a conventional electronegative atom or group. Transition/alkali metals and boron are typical elements that create partially negatively charged hydrogens. Transition-metal (M) complexes involving M-$H\cdots H–B$ types of interaction are already in the front line of theoretical and experimental investigations.[18–25] Such dihydrogen bonds were identified in several x-ray crystal structures,[17,26,27] in solution,[28,29] and the gas phase.[30–32] Like conventional H bonds, the dihydrogen bond is gaining attention because of its role in the synthesis of supermolecules, reactivity, and selectivity in solution, gas phase, and in solid state, and in designing catalysts for asymmetric hydrogenation. Some attempts have also been made to investigate dihydrogen bonding exhibited by molecules involving main group elements, such as LiH, HBeH, BH_3, AlH_3.[20,33–41] Recently Custelcean and Jackson[42] reviewed the energetic and geometric aspects of various dihydrogen bonds.

Several structural and energetic similarities have been observed between the conventional H bond and the dihydrogen bond. The noncovalently bonded $H\cdots H$ distances in $M–H\cdots H–X$ (M = transition metals, B, Li, etc.) systems typically range from 1.7 to 2.4 Å—similar to $H\cdots Y$ distances in conventional H bonds. The heats of interaction for these systems also lie within the range of typical H bonds, viz. 3–10 kcal/mol. The linearity of normal H bonds (i.e., the $X\cdots H–Y$ angle is close to 180°) is also preserved in unconventional H bonds. The $H\cdots H–X$ angles generally lie within 160–180°. However, the $M–H\cdots H$ angles are found to be strongly bent, falling in the range of 95–130°.

The first theoretical investigation on dihydrogen bonding of the H_3BNH_3 dimer by Richardson *et al.*[17] showed that the structure is cyclic and of C_2 symmetry, with two $B–H\cdots H–N$ bonds. Popelier[43] studied a particular structure

[a]Author to whom correspondence should be addressed. Tel.: 1-435-797-7230; Fax: 1-435-797-3390; Electronic mail: tapaskar@cc.usu.edu

(C_s symmetry) of $(H_3BNH_3)_2$ with three B–H···H–N bonds, two of which are identical due to the presence of a mirror plane. Using the theory of ''atoms in molecules,'' they found two dihydrogen bonds that differ in strength. Cramer and Gladfelter[44] further extended the investigation by comparing dimers of H_3BNH_3, H_3AlNH_3, and H_3GaNH_3. Using extended levels of theory, they found the C_{2h} structure of $(H_3BNH_3)_2$ to be the global minimum, whereas the other dimers have C_2 symmetry. Further, the H-bond energy decreases from boron to gallium in this series.

Most of the systems involving M–H···H–N bonds considered so far contain sp^3 hybridized N and M (A=B, Al, etc.). Very recently, Aime and co-workers[29,45,46] reported Os–H···H–N bonds where imine ligands (such as HN=CPh_2 and HN=$CHCH_3$) are coordinated with an osmium complex. Different H···H distances have been reported by these authors, such as 1.79 Å in the crystal structure (x-ray data) and 2.00 Å in solution (NMR data). A similar DHB bond is slightly longer in other amine complexes.[29,47] They also observed that the dihydrogen bond distance strongly depends on the polarity of the solvent.[29] They concluded that, when typical H bonds are not present, weaker unconventional dihydrogen bonds become important in driving the stereochemistry of the complexes. Other examples[26,48] of dihydrogen bonds such as Ir–H···H–N also seems to have sp^2 nitrogens because of planarity at N due to delocalization of lone pairs. Thus it looks as though dihydrogen bonds, where the proton donors (=N–$H^{\delta+}$) are sp^2 hybridized, also play an important role similar to their sp^3 counterparts. However, the influence of the hybridization on several aspects, such as structure, energetics, etc., of dihydrogen bond is still unknown.

In the present investigation, we explore the possibility of dihydrogen bond formation in compounds where both B and N are sp^2 hybridized. In addition we also consider complexes arising from the combination of different types of hybridized H_nBNH_n molecules, where $n=3$ (sp^3) and 2 (sp^2) forming B–H···H–N bond(s). Complex formation of H_nBNH_n molecules with ammonia via conventional N–H···N bond has also been studied for the purpose of comparison. Along with the energetic aspects of the interaction, structural and spectroscopic markers are computed using a high level of theory.

METHOD OF CALCULATIONS

The structures of the monomers and complexes studied herein are obtained at the level of Møller–Plesset perturbation theory (MP2) with frozen core approximation.[49] Dunning's correlation-consistent polarized valence-double-zeta (aug-cc-pVDZ) basis set[50,51] augmented by diffuse functions is used throughout. A previous investigation[44] indicated that this basis set, without diffuse functions, is quite adequate to describe the structure and stability of dihydrogen bonds involving boron and nitrogen atoms. Geometries are fully optimized without any symmetry constraints. Vibrational analyses at the same level [MP2(FC)/aug-cc-pVDZ] have been performed to identify true minima. Interaction or dimerization energies (ΔE) are obtained as the difference between the energies of the complex and monomer units, and corrected for basis set superposition error (BSSE) via the standard counterpoise method.[52] The energy of dihydrogen bonds (E_{DHB}) is estimated by dividing ΔE by the number of such H···H bonds in the complex. Charges on individual atoms were calculated using natural population scheme.[53] All calculations have been carried out using the GAUSSIAN98 (Ref. 54) package of *ab initio* codes. Total interaction energies were decomposed via the Kitaura–Morokuma scheme[55] as implemented in the GAMESS program.[56] Electron densities and their shifts were displayed using MOLDEN program.[57]

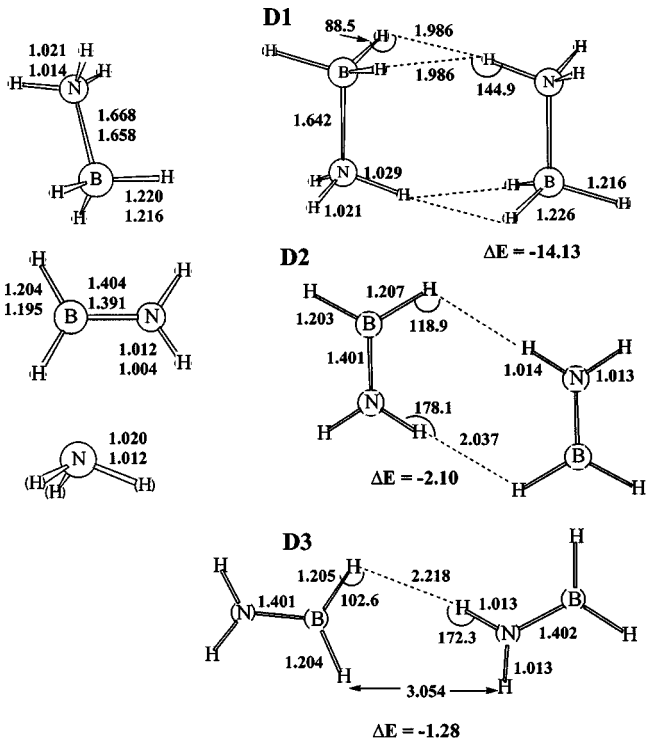

FIG. 1. Geometric parameters (in Å and degrees) of monomers and dimers of H_3BNH_3 (**D1**) and H_2BNH_2 (**D2** and **D3**), along with interaction energies (ΔE in kcal/mol). The second set of values corresponds to the experimental geometries.

RESULTS AND DISCUSSION

H_3BNH_3 and H_2BNH_2 dimers

Calculated and available experimental geometric parameters of the monomers are displayed in Fig. 1. For the monomers, MP2 predicts bonds slightly longer than experiment [H_3BNH_3,[58–60] H_2BNH_2,[61–63] and NH_3 (Ref. 64)]. The BN bond length of H_2BNH_2 is significantly shorter than that of H_3BNH_3, indicating double bond character in the former. The NH distance in sp^3 hybridized H_3BNH_3 is close to that of ammonia, and this bond contracts as the hybridization changes from sp^3 to sp^2. The BH bond length also shrinks, and the change is more pronounced compared to NH bonds.

The H_3BNH_3 dimer (**D1**), as shown in Fig. 1, exhibits four equivalent H···H bonds involving one N–H hydrogen and two B–H hydrogens of each monomer. The same structural arrangement of $(H_3BNH_3)_2$ had been reported earlier by Cramer and Gladfelter[44] using the cc-pVDZ basis set. In

TABLE I. Vibrational frequencies[a,b] (ν) of the monomers, their shift ($\Delta\nu^a$), and changes in bond lengths (Δr) caused by complexation.

ν and $\Delta\nu$ (cm^{-1})	B–N	B=N	N(sp^3)–H as/s	N(sp^2)–H as/s	B(sp^3)–H as/s	B(sp^2)–H as/s	NH_3 as/s
H_3BNH_3	651		3610/3470		2536/2473		
	608 or 968		3386/3337		2415/2340		
H_2BNH_2		1345		3728/3610		2693/2609	
		1337		3534/3451		2564/2495	
NH_3							3636/3480
							3494/3337
D1	66		−67/−84		−52/−31		
D2		16		−19/−20		−10/−11	
D6	29	11	−30/−20	−44/−74	−21/−13	−15/−16	
D7	40		−71/−178		−41/−24		−32/−18
D12		15		−44/−123		−28/−22	−12/−7
D11							−39/−33
Δr (Å)							
D1	−0.026		0.008		0.006		
D2		−0.003		0.002		0.003	
D6	−0.012	−0.002	0.003	0.007	0.003	0.003	
D7	−0.018		0.013		0.005		0.003
D12		−0.004		0.009		0.003	0.001
D11							0.004

[a]as and s stand for asymmetric and symmetric stretching frequencies, respectively.
[b]The underlined frequencies correspond to experimental values.

the present investigation additional diffuse functions were added to the cc-pVDZ basis set to better describe negatively charged nitrogen atoms. Addition of diffuse functions in the basis set (aug-cc-pVDZ) causes slight lengthening of all bonds except B–N, and the bond angles remain almost unchanged.

Dihydrogen bond formation of H_3BNH_3 is accompanied by minor lengthening of participating B–H (by 6.0 mÅ) and N–H bonds (by 8.0 mÅ) (see Table I), and significant shortening of the B–N bond by 26.0 mÅ. The HBH (114.0°) and HNH (107.7°) bond angles of H_3BNH_3 remain almost unchanged. The dihydrogen bond distance in H_3BNH_3 is 1.986 Å and the BSSE corrected interaction or dimerization energy (ΔE) is −14.1 kcal/mol. Thus each H···H dihydrogen bond between N(sp^3)–$H^{\delta+}$ and $H^{\delta-}$–B(sp^3) is assigned an energy of 3.5 kcal/mol.

Two different structures were investigated for the H_2BNH_2 dimer where both B and N atoms are sp^2 hybridized. Dimer **D2**, where two H_2BNH_2 units are placed side by side with roughly antiparalled BN bonds, forms two equivalent H···H bonds. The second possible head-to-tail structure (**D3**) exhibits a single dihydrogen bond. [A third structure (not shown) containing two equivalent H···H bonds in head-to-tail arrangements has one negative frequency, and the dihydrogen bond distance of 2.5 Å is larger than the typical range of 1.7–2.4 Å in M–H···H–X.] The H···H distance of 2.037 Å in **D2** indicates that this dimer can be classified as a dihydrogen bonded system. This complex also exhibits bond angles characteristic of unconventional H bonds: almost linear N–H···H and highly bent B–H···H bond. The NH and BH covalent bonds stretch marginally, relative to the monomers, by 1.0–3.0 mÅ. The H···H distances in **D3** differ significantly, one being only slightly longer then the typical R(H···H) of 2.2 Å. The other HH distance of 3.05 Å suggests a nonbonding contact.

The change of hybridization from sp^3 to sp^2 causes significant lowering in dimerization energy. The ΔE value is only −2.1 kcal/mol for structure **D2**, which exhibits two equivalent H···H bonds. Thus each dihydrogen bond has an energy of about 1.0 kcal/mol, which is about one-third that of sp^3 hybridized **D1**. The E_{DHB} of singly H···H bonded **D3** is found to be 1.3 kcal/mol, which is close to that of **D2**. The H···H distance of **D1** is elongated by 0.05 Å in **D2** and 0.23 Å in **D3**, and this lengthening may not be attributed solely to the change of hybridization. The other factor involved is the number of such dihydrogen bonds: four in **D1**, two in **D2**, and one in **D3**. As the number of attractive interactions between $N^{\delta-}$–$H^{\delta+}$ and $H^{\delta-}$–$B^{\delta+}$ increases, the monomers come closer.

Several different dihydrogen bonded HBNH (sp hybridized) dimers have been considered: antiparallel (similar to D2 structure), head to tail, L shape [<B–H···H(N) = 90.0°], and a bent form where <B–H···H(N) varied from 90 to 130°. In all these cases, the HH interaction is repulsive and it appears that sp hybridized HBNH does not dimerize via H···H bonds. HBNH prefers to dimerize via a B_2N_2 ring and the dimerization energy is more than −50.0 kcal/mol. Similar four-membered B_2N_2 ring structure[65] of sp^2 hybridized $(H_2BNH_2)_2$ is also stable and the dimerization energy is much higher (by about 16.0 kcal/mol) than the most stable dihydrogen bonded structure **D2**.

Mixed dimers

The first mixed dimer considered is the combination of sp^3 and sp^2 hybridized monomers, i.e., H_3BNH_3–H_2BNH_2. Both of the monomers contain N–$H^{\delta+}$ as well as B–$H^{\delta-}$ units to form H···H bonds. Thus three different dihydrogen bonded structures can be constructed form these monomers, illustrated in Fig. 2. In dimer **D4**, a single N–H···H–B DHB

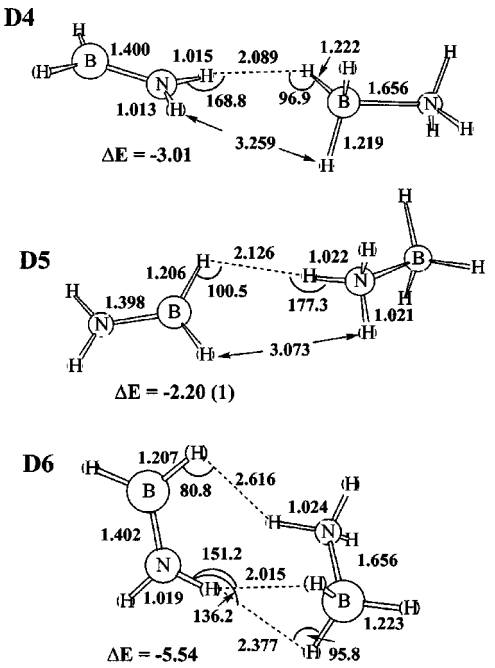

FIG. 2. Geometric parameters (in Å and degrees) and interaction energies (ΔE in kcal/mol) of different isomers of $H_3BNH_3-H_2BNH_2$ complexes. Numbers of negative frequencies are given in parentheses.

bond is formed between the NH of H_2BNH_2 and HB of H_3BNH_3, i.e., sp^2(NH)$-sp^3$(HB) combination. In dimer **D5**, both the monomers of **D4** are inverted making sp^3-sp^2 combination of N–H (H_3BNH_3) and H–B (H_2BNH_2), respectively. In the last case (**D6**), multiple DHB bonds are formed between the monomers, similar to the dimer of H_3BNH_3 and H_2BNH_2 as shown in Fig. 1.

Dimers **D4** and **D5** each exhibit a single H···H bond and the R(H···H) is shorter by 0.13 and 0.09 Å than that of singly H···H bonded sp^2 hybridized $(H_2BNH_2)_2$ (**D3**), respectively. (It may be noted that **D5** has a negative frequency of $-8.0\ cm^{-1}$ and is thus not a true minimum on the PES.) Of the three single H···H bonded dimers (**D3**–**D5**), the strongest dihydrogen bond (3.0 kcal/mol) is found in **D4** where NH is sp^2 and BH is sp^3 hybridized. The E_{DHB} value is lowered by 0.8 kcal/mol in the reverse situation, and the weakest of the three single H···H bonds is found in purely sp^2 hybridized **D3**. Like the conventional X-H···Y H bonds, a near linear relationship exists between R(H···H) and E_{DHB}; as the distance decreases, the dihydrogen bond gets stronger.

The most stable mixed $H_3BNH_3-H_2BNH_2$ dimer is **D6** with three close H···H distances. Such different H–H distances have also been observed by Patawari *et al.*[32] in phenol-aniline complexes. The shortest distance of 2.015 Å between N(sp^2)–H and one of the H–B(sp^3) fall in the range of a typical dihydrogen bond. The second HH distance involving the same groups is only slightly shorter than the upper limit of typical H···H distance of 2.4 Å. The distance between N(sp^3)–H and H–B(sp^2) is much longer (~0.2 Å) than the limiting value and thus should not be considered a dihydrogen bond. Because of nonequivalent H···H bonds in this dimer, it is difficult to assign a single dihydrogen bond energy. However, as a crude approximation, out of the −5.5 kcal/mol total, about −3.0 kcal/mol is attributed to the shortest H···H bond. This estimate was made by comparing HH distances between **D4** and **D6** and their E_{DHB}. The rest ~−2.5 kcal/mol comes from the other H–H attractive interactions, where the N(sp^3)–H and H–B(sp^2) interaction may have some contribution despite long HH separation. In fact the interaction energy of **D6** lowers from −5.54 to −4.94 kcal/mol when hydrogens of (HB)H and H(NH_2) are further separated by 1.0 Å from the optimized value of 2.616 Å, while keeping other geometric parameters, directly involved in H···H bonds in **D6**, almost the same. Thus an energy of about −0.6 kcal/mol seems sensible for such a long H···H interaction. It is worth mentioning that the concerned hydrogen is closer to the BN double bond.

The N–H and B–H bonds involved directly in H···H bonds stretch, relative to monomers, by 2–7 mÅ. Single B–N bond in all three mixed dimers shrink (by 7–12 mÅ) upon dimerization but to a lesser extent compared to that of $(H_3BNH_3)_2$. The contractions of the B═N bond are minimal compared to B–N single bonds. The BH···H and NH···H angles in mixed dimers lie within the 80–100° and 136–177° ranges, respectively.

It can be seen that NH of sp^2 hybridized H_2BNH_2 forms a stronger DHB compared to its sp^3 counterpart. On the other hand, dihydrogen bond involving B(sp^3)–H is stronger than that of B(sp^2)–H.

Complexes with NH_3

Several possible combinations of H_nBNH_n ($n=3$ and 2) with NH_3 via both dihydrogen and conventional H bond were considered. Four arrangements have been investigated for both $H_3BNH_3-NH_3$ (**D7**–**D10**) and $H_2BNH_2-NH_3$ (**D12**–**D14**) and these dimers are shown in Figs. 3 and 4, respectively. For the sake of comparison, the N–H···N H-bonded ammonia dimer (**D11** in Fig. 3) was also studied.

Complete geometry relaxation during optimization of $H_3BNH_3-NH_3$ leads to the **D7** structure, where both dihydrogen and regular H bonds exist. In this dimer the NH_3 molecule acts as both proton acceptor as well as donor. A similar structure for $H_3BNH_3-NH_3$ was obtained by Li *et al.*[66] using MP2/6-31++G**. The H···H distance of 2.5 Å is beyond the typical limit for a dihydrogen bond. However, a distance of 2.4 Å between the OH proton and the Ir–H has been reported by Stevenes *et al.*[67] (It may be noted that the MP2 distances are slightly longer than the experimental values.) The interaction energy of −8.7 kcal/mol was reduced to −7.0 kcal/mol when the dihydrogen bonds of **D7** were removed, as shown in **D8**. The R(H···N) lengths in **D7** and **D8** are very close, while the R(NN) distance increases by about 0.08 Å in **D8**. The major change is found in the opening of the N–H···N bond angle in **D8** by about 27°, compared to **D7**. The energy cost of a similar reorientation in $(NH_3)_2$ is found to be less than 0.5 kcal/mol.[4] Thus the two H···H bonds of **D7** appear to contribute a small fraction of the total interaction energy, despite the large HH separation.

Compared to ammonia dimer (**D11**), the interaction en-

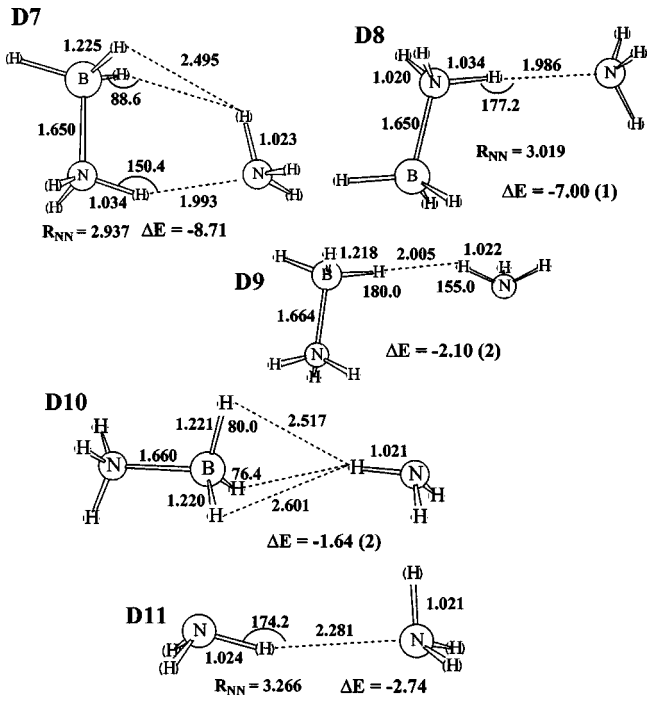

FIG. 3. Geometric parameters (in Å and degrees) and interaction energies (ΔE in kcal/mol) of different isomers of $H_3BNH_3-NH_3$ complexes. Numbers of negative frequencies are given in parentheses.

ergy of regular H-bonded complexes of $H_3BNH_3-NH_3$ (**D7** and **D8**) is quite high. The presence of electron deficient–BH_3 makes H_3BNH_3 a much stronger proton donor. R(NN) decreases in the order **D11**$\gg$**D8**$>$**D7**, and the interaction energy follows the reverse pattern. A nearly linear relationship exists between R(NN) and ΔE, similar to that commonly observed in conventional H bonds.[4]

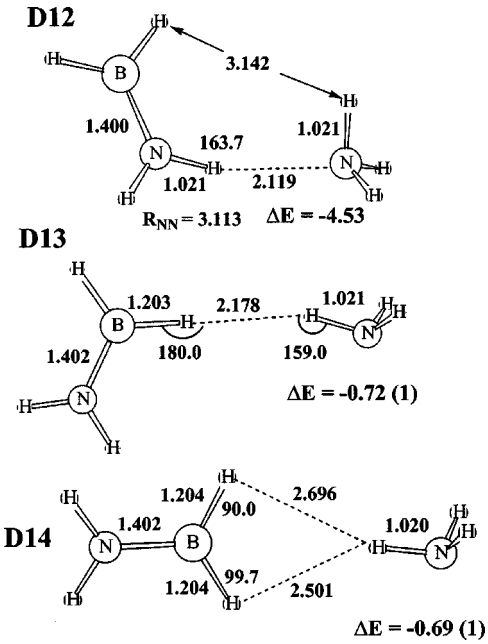

FIG. 4. Geometric parameters (in Å and degrees) and interaction energies (ΔE in kcal/mol) of different isomers of $H_2BNH_2-NH_3$ complexes. Numbers of negative frequencies are given in parentheses.

The single H···H bonded structure **D9**, between H_3BNH_3 and NH_3, was obtained by freezing the B–H···H angle at 180.0°. It may be noted that this structure is not a local minimum. Nevertheless this interaction is attractive and the interaction energy is -2.1 kcal/mol. The effect of the B–H···H angle on R(H···H) and interaction energy of single dihydrogen bonded $H_3NBH_3-NH_3$ has been studied by varying $<$B–H···H from 80° (**D10**) to 220° via 180.0° (structure as shown in **D9**). Except R(H···H), all other geometric parameters were kept constant as obtained in **D9** and the N–H···H angle was fixed at 170.0°. Moving ammonia from **D10** arrangement to **D9**, has practically no effect (less than 0.5 kcal/mol) on total interaction energy. The energy variation with B–H···H angle crosses through two minima at 100.0 and 180.0°. The H···H distance remains almost unchanged until the B–H···H angle reaches 120°, after which further bending of this bond causes stretching of R(H···H). Moving of NH_3 molecule in the other direction (i.e., towards the other nitrogen) lowers the E_{DHB}; the maximum change of about 1.3 kcal/mol occurs at 220.0 and the R(H···H) value changes marginally.

The most stable structure of $H_2BNH_2-NH_3$ is **D12** (as shown in Fig. 4). The interaction energy of -4.5 kcal/mol originates primarily from the conventional N–H···H–H bond. This H-bond energy is almost half of that of $H_3BNH_3-NH_3$ (**D7**). However, it is stronger than that of the ammonia dimer (**D11**). The NN and H···N distances of **D12** are almost intermediate between **D7** and **D11**. Similar to **D7**, one of the hydrogens of NH_3 of **D12** is oriented towards one of the H atoms of BH_2. However, the distance of 3.14 Å is too long to designate it as dihydrogen bond. Single dihydrogen bonded $H_2BNH_2-NH_3$ (**D13**) was obtained by fixing B–H···H angle at 180.0°. The H···H bond energy is less than 1.0 kcal/mol. Dependence of R(H···H) and dihydrogen bond energy on the B–H···H angle is verified by varying this angle from 90° (**D14**) to 220°. The N–H···H angle was kept fixed at 170.0°. The dihydrogen bond energy is even less sensitive on such wide variation of $<$B–H···H, compared to its sp^3 correlate. However, one minimum in the PES is located at 100.0°. The H···H distance remains close to 2.2 Å until the angle reaches 120.0°. Further motion of ammonia towards the other hydrogen of BH_2 (one such structure is **D14**) causes larger separation between proton donor and acceptor.

Electron density shift

Upon classical H-bond formation, a certain amount of electron density transfers from the proton acceptor to the donor molecule.[4] In addition, there are some rearrangements of density within the confines of each monomer. In this section, we compare the electronic changes that accompany the formation of the dihydrogen bond with those within a conventional H bond. In order to avoid the arbitrariness of population analysis schemes to assign charge to various nuclei, maps of electron density shift in the entire space of the complex are used.

The shifts of electron density that result from the formation of the classical H bond in ammonia dimer (**D11**) are illustrated in Fig. 5. This map has been generated, point by

FIG. 5. (Color) Shifts of electron density occurring in ammonia dimer as a result of formation of the complex. Blue region denotes gain, and red regions represent loss. Contour illustrated corresponds to change by 0.001 au.

point in space, by taking the difference between the densities in the dimer and isolated monomers. Blue regions of Fig. 5 represent the accumulation of additional electron density as a result of H-bond formation; red regions indicate loss of density. The most common feature of conventional H-bond formation includes the red region that surrounds the bridging hydrogen atom, consistent with the well-established notion that this bridging hydrogen loses density. The regions of charge buildup on the near side of the proton acceptor, between bridging hydrogen and nitrogen, and peripheral regions of the donor molecule are also common for typical H bonds. The overall charge transfer from proton acceptor to donor is about 0.014 electrons, as measured by natural population analysis.

The density difference plots of $(H_3BNH_3)_2$ and $(H_2BNH_2)_2$ are shown in Fig. 6. In both cases, each monomer behaves as donor and acceptor at the same time; hydrogen(s) of BH_n unit acts as proton acceptor and NH_n donates

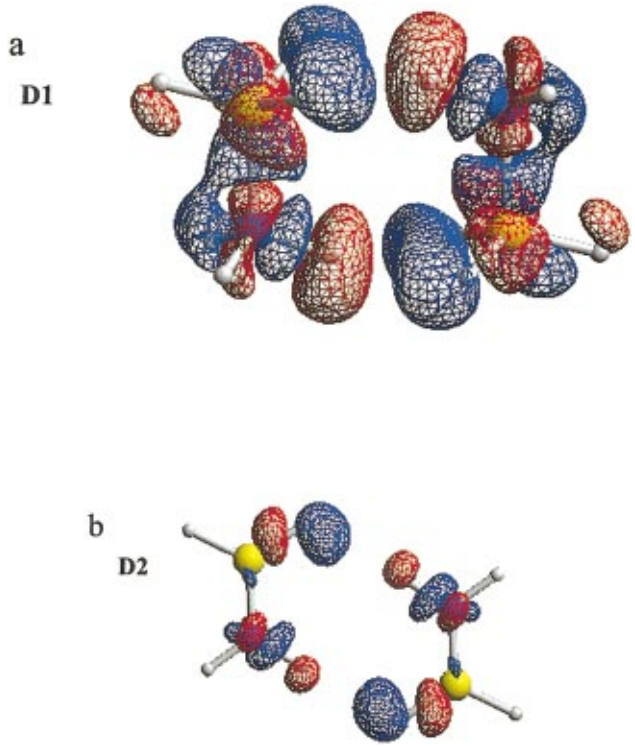

FIG. 6. (Color) Shifts of electron density occurring in $(H_3BNH_3)_2$ (a) and $(H_2BNH_2)_2$ (b) dimers as a result of formation of the complex. Contours illustrated correspond to change by 0.001 au.

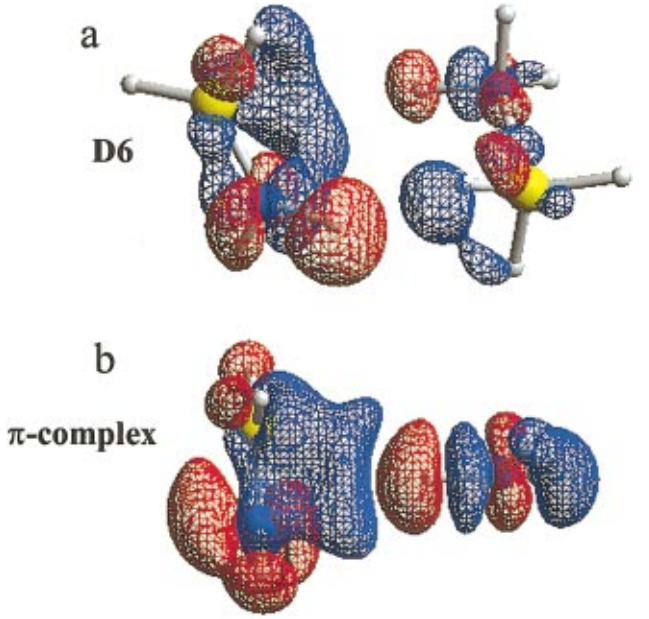

FIG. 7. (Color) Shifts of electron density occurring in $H_3BNH_3-H_2BNH_2$ complex (a) and $H_2BNH_2-NH_3$ π complex (b) as a result of formation of the complex. Contours illustrated in (a) and (b) corresponds to change by 0.001 and 0.0002 au, respectively.

proton(s). Thus overall charge transfer from one monomer to other is nullified by equivalent numbers of dihydrogen bond formation. As in the case of the classical N–H···N bond, the bridging NH proton of both monomers loses density (red regions). The blue regions near the proton acceptor BH hydrogens are similar to that of the acceptor nitrogen in ammonia dimer. In general, the patterns of gain and loss of electron density are qualitatively similar for both types of H bonds. Differences of magnitude of charge build up and depletion are very roughly proportional to the interaction energies of each complex.

The same pattern extends to the mixed dimers, wherein one of the monomers is sp^3 hybridized while the other is sp^2. The density difference between the most stable mixed dimer **D6** and constituent monomers, with more than one dihydrogen bond, is plotted in Fig. 7(a). Since these H···H bonds are not equivalent, as in the cases of $(H_3BNH_3)_2$ and $(H_2BNH_2)_2$, the sizes of the blue regions of charge gain near proton acceptor hydrogens of BH_n are also different. The pattern around the H_3BNH_3 molecule in mixed dimer **D6** is similar to that in the H_3BNH_3 dimer **D1**. Similarly, the H_2BNH_2 patterns in **D6** and **D2** are also not very different. The charge shift from the sp^2 monomer to the sp^3 is only 1.0 millielectron (me) as measured by natural population analysis.

In order to examine the possibility of a π–hydrogen bond, the $H_2BNH_2-NH_3$ [Fig. 7(b)] complex has been arranged such that the H–N bond of ammonia approaches the B═N double bond of H_2BNH_2 from above. The optimized distance between the hydrogen and the mid-point of the BN double bond is 2.65 Å, close to that found in **D6**. The density difference plot of this complex is illustrated in Fig. 7(b). It can be clearly seen that the blue region, build up near the B═N bond, extends toward the proton, which is a charac-

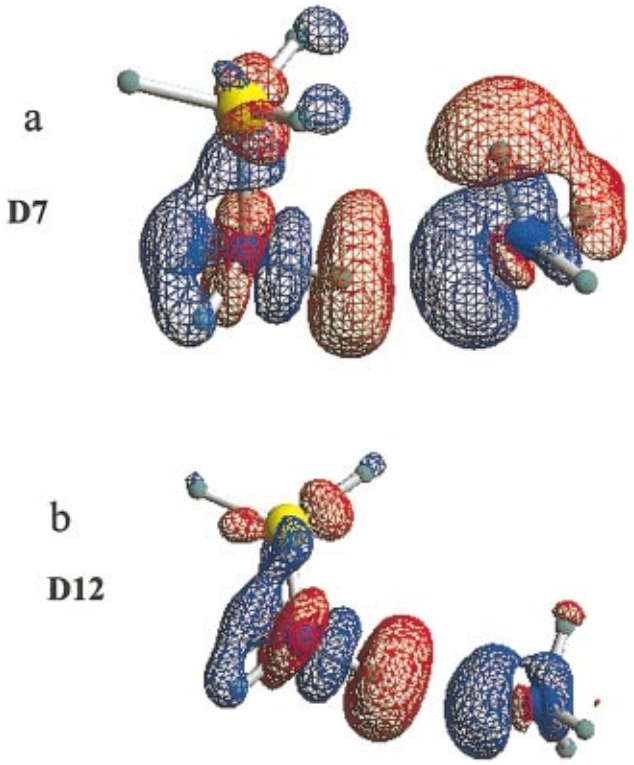

FIG. 8. (Color) Shifts of electron density occurring in $H_3BNH_3-NH_3$ complex (a) and $H_2BNH_2-NH_3$ (b) as a result of formation of the complex. Contours illustrated correspond to change by 0.001 au.

teristic feature of H bonds and the bridging H suffers the usual density loss. The interaction energy between H_2BNH_2 and NH_3 in this structural form is -1.5 kcal/mol (without BSSE correction). Thus the possibility of π-hydrogen bond formation cannot be ruled out.

These characteristics of charge shifts upon H-bond formation are also charecteristic of the $H_3BNH_3-NH_3$ and $H_2BNH_2-NH_3$ complexes, as shown in Fig. 8. It was mentioned in the previous section that $H_3BNH_3-NH_3$ is the only complex where NH_3 acts as both acceptor and donor, at the same time. The red region [as shown in Fig. 8(a)] around the hydrogen of NH_3, facing the BH_3 segment, further supports this fact. The loss of charge on the same H atom of the sp^2 complex [Fig. 8(b)] is insignificant compared to that of its sp^3 counterpart. In both complexes, the proton acceptor ammonia loses charge: 39 me in **D7** and 26 me in **D12**.

Spectroscopic features

Vibrational frequencies of the monomers and the complexes were calculated at the MP2/aug-cc-pVDZ level and the results are summarized in Table I, along with available experimental frequencies.[58,59,63] The major discrepancy between theory and experiment occurs in the stretching vibration ν(B–N) of H_3BNH_3. In fact, the experimental[57] B–N stretching frequency estimates vary between 608 and 968 cm^{-1}. (It is worth mentioning that the experimental IR spectra of H_3BNH_3 are somewhat complicated due to the presence of polymeric species in the effusion vapor.) The present MP2 frequency of 651 cm^{-1} is close to the former value. A value of 671 cm^{-1} has been predicted for ν(B–N) of H_3BNH_3 by MP2/6-31++G**.[66] The B═N stretching frequency of H_2BNH_2 estimated by MP2 theory is in good agreement with the experimental value (in gas phase[63]). In general, theoretical frequencies of BH and NH bonds are slightly overestimated, by a factor of about 1.049, compared to the experimental values.

The changes in BN, BH, and NH frequencies ($\Delta\nu$) and bond lengths (Δr) of the monomers upon H and dihydrogen-bond formation are summarized in Table I. The contractions of BN bonds are associated with blueshifts and the stretches of BH and NH bonds with redshifts. Contractions of the B–N bonds are more pronounced than those of B═N, and thus the blueshift of B–N observed in H_3BNH_3 complexes is larger than in sp^2 analogues. The redshift in both N(sp^3)–H (Refs. 31 and 32) and N(sp^2)–H (Ref. 46) has been recorded experimentally. However, the H–N bond of ammonia shrinks by 0.001 Å in the π complex of $H_2BNH_2-NH_3$ [see Fig. 7(b)] and a blueshift (redshift) of $+9.0$ (-8.0) cm^{-1} has been found for asymmetric (symmetric) band of N–H bond.

Energy decomposition

A breakdown of the molecular interaction energy into a number of components can offer insight into the fundamental nature of the interaction. One popular means of such decomposition is via an approach attributed to Kitaura and Morokuma[55] in which the electrostatic energy (ES) represents the classical Coulombic force between the charge distributions of the two partner molecules. The exchange energy (EX) is associated with the steric repulsion that arises from the overlap of the monomer charge clouds. The remaining components arise when the two molecules are permitted to perturb the electron clouds of one another. The polarization (POL) and charge transfer (CT) contributions represent the energetic consequences of electronic redistributions that occur within the confines of a single molecule and those that cross from one molecule to the other, respectively. The mixing term (MIX) or higher order coupling arises from the failure of the above four terms to fully account for all aspects of the interaction. Finally, the correction component to the interaction energy (CORR) contains dispersion as its major contributor as well as additional factors.

The energy components to the interaction energies of the different complexes studied herein are reported in Table II. (It may be noted that the sums of these components are slightly higher than the total interaction energies shown in Figs. 1–4, due to the basis set superposition correction to the interaction energies reported in the figures) For the sake of comparison, conventionally H-bonded ammonia dimer is also included in the table. Inspection of the data in the last column (**D11**) reiterates the generally accepted notion that the conventional H bond is largely electrostatic in origin, with much smaller attractive contributions from polarization, charge transfer, and dispersion. Exchange repulsion is comparable, although smaller in magnitude, to ES, and of opposite sign. The sum of ES and EX terms is slightly attractive (-0.26 kcal/mol). The dipole–dipole interaction is only 15% of the full ES suggesting it furnishes a very poor ap-

TABLE II. Decomposition elements[a] (kcal/mol) of interaction energies of complexes,[b] calculated with aug-cc-pVDZ basis set.

	D1	D2	D6	D7	D12	D11
ES	−19.59	−2.68	−7.79	−15.14	−8.14	−5.15
Dip–dip[c]	−13.67	−0.62	−1.45	−4.39	−1.42	−0.80
EX	17.73	4.47	8.77	13.69	7.99	4.89
ES+EX	−1.86	1.79	0.98	−1.45	−0.15	−0.26
POL	−14.63	−0.95	−4.23	−5.45	−1.95	−0.92
CT	−6.54	−1.50	−2.81	−3.98	−2.17	−1.20
MIX	13.01	0.74	3.79	4.37	1.37	0.51
CORR[d]	−6.16	−2.31	−3.93	−3.56	−2.93	−1.50

[a]Uncorrected for BSSE.
[b]See Figs. 1–4 for the structures.
[c]Coulombic interaction between dipoles of subunits.
[d]CORR$=\Delta E(\mathrm{MP2})-\Delta E(\mathrm{HF})$.

proximation. A small repulsive contribution arises from the MIX component.

In H_3BNH_3 dimer (**D1**), where the interaction energy resides in the four equivalent B–H···H–N dihydrogen bonds, the POL, CT, MIX, and CORR terms contribute significantly. Such high contribution from the polarization energy (75% of the ES) is connected with considerable shift in electron density within the monomers [see Fig. 6(a)]. The CT contributes about 35% of ES. (By symmetry, there is no total charge shift from one monomer to the other.) A closer look at the natural charges of the monomer reveals that 0.33 electron shifts from the H_3N unit of H_3BNH_3 to BH_3 because of the dative $H_3N\rightarrow BH_3$ bond. The amount of charge transfer within the monomers increases to 0.36*e* upon complexation. The electron correlation (CORR) term is almost of the same magnitude as CT, whereas the contribution from higher-order term (MIX) is repulsive and is almost double CORR.

The exchange repulsion of **D2** does not follow the same trend as found in conventional H bonds. In this sp^2 hybridized H_2BNH_2 dimer, the EX is significantly larger than ES. The EX of **D6** is only slightly larger than ES when one monomer is sp^2 while the other is sp^3. Thus it appears that dihydrogen bonds involving =N–H and =B–H are different from the classical H bonds. Exchange repulsion energies of **D7** and **D12** follow the similar trend as noted for ammonia dimer. The sum of ES and EX results in a positive value (repulsive) for **D2** and **D6**.

POL and CT follow different trends: for **D1**, **D6**, and **D7** POL is greater than CT, while for the rest of the complexes (**D2**, **D12**, and **D11**) this trend is reversed. The former three complexes contain H_3BNH_3, while this molecule does not occur in the latter three dimers. Similar to **D1** as described above, the geometric distortion (see Table I) and significant changes of electron density [Figs. 7(a) and 8(a)] within each monomer of **D6** and **D7** are associated with higher percentage of polarization energy contribution.

Competing effect between sp^3 and sp^2 hybridization

In the above sections, discussion was mostly concentrated on the most stable isomers of DHB and H-bonded complexes. Since those dimers are mostly associated with multiple N–H···N and N–H···H–B bonds, the competing effect between different hybridizations on such bonds may not be assessed correctly. To understand the effect of hybridization on dihydrogen and H bonds, interaction energies, geometric parameters, and vibrational frequencies of single N–H···N and N–H···H–B bonded systems are summarized in Table III.

The upper section of this table shows different properties of conventional N–H···N H-bonded complexes between sp^3 hybridized H_3BNH_3 and ammonia, and sp^2 hybridized H_2BNH_2 and ammonia. For the sake of comparison, ammonia dimer is also included. The strongest H bond is found in $H_3BNH_3-NH_3$, followed by $H_2BNH_2-NH_3$, and then $(NH_3)_2$. Thus the presence of BH_2 and BH_3 group enhances the stability of the N–H···N bond. R(H···N) distance elongates as the bond gets weaker. The stretches of donor H–N bonds are associated with redshifts. These changes are greatest in the strongest H-bonded **D8** dimer in the group, and decrease as the bond weakens.

The properties of single B–H···H–N dihydrogen bond formed by different hybridized B–H (N–H) with a common N–H (B–H) are grouped in the next section. The first group represents DHB between sp^3 and sp^2 B–H, and N–H of ammonia. As in the case of the conventional H bond, change of hybridization from sp^3 to sp^2 lowers the dihydrogen bond energy. Comparison of **D9** with **D8** and **D13** with **D12** indicates that conventional N–H···N bonds are much stronger than N–H···H–B bonds. Both sp^3 and sp^2 B–H bonds shrink and undergo a blueshift. In the case of $H_2BNH_2-NH_3$ these changes in B–H and N–H bond are less significant compared to their sp^3 counterpart.

In the next group, we compare B–H···H–N between $H_3BNH_3-H_3BNH_3$ (**D15**) and $H_2BNH_2-H_3BNH_3$ (**D4**). The single dihydrogen bonded **D15** (Fig. 9) is obtained by keeping N–H···H and B–H···H angle fixed at 160.0° and 90.0°, respectively. The DHB energy decreases as hybridization changes from sp^3 to sp^2. In fact in the subsequent groups, the single dihydrogen bond energy follows the same order. Compared to sp^3, elongation of sp^2 hybridized B–H and N–H bonds is less pronounced.

In summary, the sp^3-sp^3 combinations of B–H with H–N forms the strongest dihydrogen bonds, followed by N(sp^2)–H and H–B(sp^3) combination and then B(sp^2)–H and H–N(sp^3). The DHB interaction energy between sp^2-sp^2 combinations is weakest. Like conventional H

TABLE III. Single hydrogen and dihydrogen bond energies (ΔE) and lengths (R), and changes in BH and NH bond lengths (Δr) and their frequencies[a] ($\Delta \nu$) upon complex formation.

		ΔE (kcal/mol)	R (H···Y) or (H···H) (Å)	Δr (Å) B–H/N–H	$\Delta \nu$ (cm^{-1}) B–H (as/s)	$\Delta \nu$ (cm^{-1}) N–H (as/s)
			N–H···N–H bond			
D8	$H_3B–H_2$**N–H**···**N**H_3	−7.00	1.986	−/0.013		−71/−186
D12	$H_2B–H$**N–H**···**N**H_3	−4.53	2.119	−/0.009		−44/−123
D11	H_2**N–H**···**N**H_3	−2.74	2.281	−/0.004		−39/−33
			B–H···H–N dihydrogen bond			
D9	$H_3N–H_2$**B–H**···**H–N**H_2	−2.10	2.005	−0.002/0.002	14/8	−18/−11
D13	$H_2N–H$**B–H**···**H–N**H_2	−0.72	2.178	−0.001/0.001	5/6	−2/−1
D15	$H_3B–H_2$**N–H**···**H–B**$H_2–NH_3$	−4.26	1.953	0.005/0.003	−9/−10	−34/−19
D4	$H_2B–H$**N–H**···**H–B**$H_2–NH_3$	−3.10	2.089	0.002/0.003	−9/0	−18/−18
D5	$H_3B–H_2$**N–H**···**H–B**$H–NH_2$	−2.20	2.126	0.002/0.001	−24/−18	−9/−2
D3	$H_2B–H$**N–H**···**H–B**$H–NH_2$	−1.28	2.218	0.001/0.001	−13/−12	−4/−3
D15	$H_3N–H_2$**B–H**···**H–N**$H_2–BH_3$	−4.26	1.953	0.005/0.003	−9/−10	−34/−19
D5	$H_2N–H$**B–H**···**H–N**$H_2–BH_3$	−2.20	2.126	0.002/0.001	−24/−18	−9/−2
D4	$H_3N–H_2$**B–H**···**H–N**$H–BH_2$	−3.10	2.089	0.002/0.003	−9/0	−18/−18
D3	$H_2N–H$**B–H**···**H–N**$H–BH_2$	−1.28	2.218	0.001/0.001	−13/−12	−4/−3

[a]as and s stand for asymmetric and symmetric stretching frequencies, respectively.

bonds, stronger DHB's are associated with shorter H···H distance, and a near linear relationship exists between R(H···H) and ΔE.

CONCLUSION

Dimers of H_3BNH_3 and H_2BNH_2 have been studied using the MP2/aug-cc-pVDZ method. Two possible dihydrogen bonded structures, via one and two B–H···H–N bonds, for $(H_2BNH_2)_2$ have been theoretically characterized. The sp^2 hybridized aminoborane forms weaker B–H···H–N dihydrogen bonds. In their mixed dimer, H_2BNH_2 acts as a proton donor, while sp^3 H_3BNH_3 seems a better proton acceptor. Similar to dihydrogen bonds, the typical N–H···N–H bonds formed by sp^3 H_3BNH_3 with NH_3 are much stronger than H_2BNH_2. These trends are opposite to the case of hydrocarbons;[68] the strongest C–H···O hydrogen bond is formed by sp hybridized acetylene followed by sp^2 and then sp^3. The dimer of sp-hybridized HBNH could not be characterized because of the repulsive nature of the interaction.

The formation of dihydrogen bonds causes considerable electron density rearrangements within each monomer and these changes are more prominent in the sp^3 than sp^2 system. Basically, H···H interactions appear to be very similar to conventional N–H···H bonds with respect to shift of electron density; the bridging proton in both cases become more positive. Similar to typical H bonds, the N–H bonds have been shown to stretch and undergo a redshift in vibrational frequency upon formation of dihydrogen bond. The magnitude of the redshift is more prominent in H_3BNH_3.

A difference noted between dihydrogen and H bond is the significant contribution from polarization, charge transfer, correlation, and higher-order components of total interaction energy in the former case. The other difference between sp^2 and sp^3 systems is the higher contribution from the exchange repulsion energy than the attractive electrostatic energy in the former case.

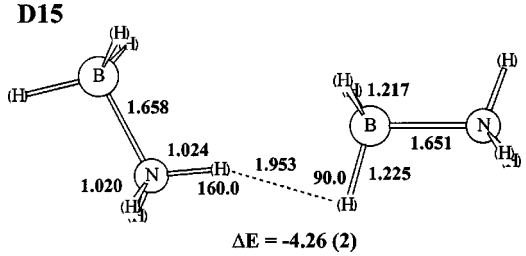

FIG. 9. Geometric parameters (in Å and degrees) of single dihydrogen bonded dimer of H_3BNH_3, along with interaction energies (ΔE in kcal/mol).

[1] G. A. Jeffrey, *An Introduction to Hydrogen Bonding* (Oxford University Press, Oxford, 1997).
[2] L. A. Curtiss and M. Blander, Chem. Rev. **88**, 827 (1988).
[3] G. A. Jeffrey and W. Saenger, *Hydrogen Bonding in Biological Structures* (Springer-Verlag, Berlin, 1991).
[4] S. Scheiner, *Hydrogen Bonding: A Theoretical Perspective* (Oxford University Press, New York, 1997).
[5] I. Alkorta, I. Rozas, and J. Elguero, Chem. Soc. Rev. **27**, 163 (1998).
[6] T.-H. Tang, W.-J. Hu, D.-Y. Yan, and Y.-P. Cui, J. Mol. Struct.: THEOCHEM **207**, 319 (1990).
[7] T. Steiner, E. B. Starikov, A. M. Amado, and J. J. C. Teixeira-Dias, J. Chem. Soc., Perkin Trans. 2 **1995**, 1321.
[8] T. E. Muller, M. P. Mingos, and D. J. Williams, J. Chem. Soc., Chem. Commun. **1994**, 1787.
[9] R. Sumathi and A. K. Chandra, Chem. Phys. Lett. **271**, 287 (1997).
[10] A. K. Chandra and M. T. Nguyen, J. Chem. Res., Synop. **1997**, 216.
[11] G. R. Desirahu and T. Steiner, *The Weak Hydrogen Bond in Structural Chemistry and Biology* (Oxford, New York, 1999).
[12] Y. Gu, T. Kar, and S. Scheiner, J. Am. Chem. Soc. **121**, 9411 (1999).
[13] S. Scheiner, in *Advances in Molecular Structure Research*, edited by M. Hargittai and I. Hargittai (JAI, Stamford, CT, 2000) Vol. 6, p. 159.
[14] S. Scheiner, T. Kar, and J. Pattanayak, J. Am. Chem. Soc. **124**, 13257 (2002).
[15] I. Rozas, I. Alkorta, and J. Elguero, J. Phys. Chem. A **101**, 4236 (1997).
[16] A. B. Sannigrahi, T. Kar, B. G. Niyogi, P. Hobza, and P. v. R. Schleyer, Chem. Rev. **90**, 1061 (1990).
[17] T. B. Richardson, D. S. Gala, R. H. Crabtree, and P. E. M. Siegbahn, J. Am. Chem. Soc. **117**, 12875 (1995).
[18] B. Chin, A. J. Lough, R. H. Morris, C. T. Schweitzer, and C. D'Agostino, Inorg. Chem. **33**, 6278 (1994).

[19] R. H. Crabtree, P. E. M. Siegbahn, O. Eisenstein, A. L. Rheingold, and T. F. Koetzle, Acc. Chem. Res. **29**, 348 (1996).
[20] Q. Liu and R. Hoffmann, J. Am. Chem. Soc. **117**, 10108 (1995).
[21] B. P. Patel, K. Kavallieratos, and R. H. Crabtree, J. Organomet. Chem. **528**, 205 (1997).
[22] G. Orlova, S. Scheiner, and T. Kar, J. Phys. Chem. A **103**, 514 (1999).
[23] E. S. Shubina, E. V. Bakhmutova, A. M. Filin, I. B. Sivaev, L. N. Teplitskaya, A. L. Chistyakov, I. V. Stankevich, V. I. Bakhmutov, V. I. Bregadze, and L. M. Epstein, J. Organomet. Chem. **657**, 155 (2002).
[24] R. H. Crabtree, Mod. Coord. Chem. **2002**, 31.
[25] Y. F. Lam, C. Yin, C. H. Yeung, S. M. Ng, G. Jia, and C. P. Lau, Organometallics **21**, 1898 (2002).
[26] E. Peris, L. J. C. J. E. Rambo, O. Eisenstein, and R. H. Crabtree, J. Am. Chem. Soc. **117**, 3485 (1995).
[27] W. T. Klooster, T. F. Koetzle, P. E. M. Siegbahn, T. B. Richardson, and R. H. Crabtree, J. Am. Chem. Soc. **121**, 6337 (1999).
[28] E. S. Shubina, N. V. Belkova, A. N. Krylov, E. V. Vorontsov, L. M. Epstein, D. G. Gusev, M. Niedermann, and H. Berke, J. Am. Chem. Soc. **118**, 1105 (1996).
[29] S. Aime, M. Ferriz, R. Gobetto, and E. Valls, Organometallics **19**, 707 (2000).
[30] G. Naresh Patwari, T. Ebata, and N. Mikami, J. Chem. Phys. **113**, 9885 (2000).
[31] G. Naresh Patwari, T. Ebata, and N. Mikami, J. Chem. Phys. **114**, 8877 (2001).
[32] G. Naresh Patwari, T. Ebata, and N. Mikami, J. Chem. Phys. **116**, 6056 (2002).
[33] M. Remko, Mol. Phys. **94**, 839 (1998).
[34] S. A. Kulkarni, J. Phys. Chem. A **102**, 7704 (1998).
[35] S. A. Kulkarni, J. Phys. Chem. A **103**, 9330 (1999).
[36] S. A. Kulkarni and A. K. Srivastava, J. Phys. Chem. A **103**, 2836 (1999).
[37] S. J. Grabowski, Chem. Phys. Lett. **312**, 542 (1999).
[38] S. J. Grabowski, Chem. Phys. Lett. **327**, 203 (2000).
[39] S. J. Grabowski, J. Mol. Struct. **553**, 151 (2000).
[40] S. J. Grabowski, J. Phys. Chem. A **104**, 5551 (2000).
[41] S. J. Grabowski, Chem. Phys. Lett. **338**, 361 (2001).
[42] R. Custelcean and J. E. Jackson, Chem. Rev. **101**, 1963 (2001).
[43] P. L. A. Popelier, J. Phys. Chem. A **102**, 1873 (1998).
[44] C. J. Cramer and W. L. Gladfelter, Inorg. Chem. **36**, 5358 (1997).
[45] S. Aime, M. Ferriz, R. Gobetto, and E. Valls, Organometallics **18**, 2030 (1999).
[46] S. Aime, E. Diana, R. Gobetto, M. Milanesio, E. Valls, and D. Viterbo, Organometallics **21**, 50 (2002).
[47] S. Aime, R. Gobetto, and E. Valls, Organometallics **16**, 5140 (1997).
[48] J. C. Lee, E. Peris, A. L. Rheingild, and R. H. Crabtree, J. Am. Chem. Soc. **116**, 11014 (1994).
[49] J. A. Pople, R. Seeger, and R. Krishnan, Int. J. Quantum Chem., Quantum Chem. Symp. **11**, 149 (1977).
[50] T. H. Dunning, Jr., J. Chem. Phys. **90**, 1007 (1989).
[51] D. E. Woon and T. H. Dunning, Jr., J. Chem. Phys. **98**, 1358 (1993).
[52] S. F. Boys and F. Bernardi, Mol. Phys. **19**, 553 (1970).
[53] A. E. Reed, R. B. Weinstock, and F. J. Weinhold, J. Chem. Phys. **83**, 735 (1985).
[54] M. J. Frisch, G. W. Trucks, H. B. Schlegel *et al.* GAUSSIAN 98, Gaussian, Inc., Pittsburgh, PA, 1998.
[55] K. Kitaura and K. Morokuma, Ont. J. Quantum Chem. **10**, 325 (1976).
[56] M. W. Schmidt, K. K. Baldridge, J. A. Boatz, S. T. Elbert, M. S. Gordon, J. H. Jensen, S. Koseki, N. Matsunaga, and K. A. Nguyen, J. Comput. Chem. **14**, 1347 (1993).
[57] G. Schaftenaar, CAOS/CAMM Center Nijmegen, The Netherlands, 1991.
[58] J. Smith, K. S. Seshadri, and D. White, J. Mol. Spectrosc. **45**, 327 (1973).
[59] J. D. Carpenter and B. S. Ault, Chem. Phys. Lett. **197**, 171 (1992).
[60] L. R. Thorne, R. D. Suenram, and F. J. Lovas, J. Chem. Phys. **78**, 167 (1983).
[61] M. Sugie, H. Takeo, and C. Matsumura, Chem. Phys. Lett. **64**, 573 (1979).
[62] M. Sugie, H. Takeo, and C. Matsumura, J. Mol. Spectrosc. **123**, 286 (1987).
[63] J. D. Carpenter and B. S. Ault, J. Phys. Chem. **1991**, 3502.
[64] W. Hehre, L. Radom, P. v. R. Schleyer, and J. A. Pople, *Ab Initio Molecular Orbital Theory* (Wiley, New York, 1986).
[65] D. R. Armstrong and P. G. Perkins, J. Chem. Soc. A **1970**, 2748.
[66] J. Li, F. Zhao, and F. Jing, J. Chem. Phys. **116**, 25 (2002).
[67] R. C. Stevenes, R. Bau, D. Milstein, O. Blum, and T. F. Koetzle, J. Chem. Soc. Dalton Trans. **1990**, 1429.
[68] S. Scheiner, S. J. Grabowski, and T. Kar, J. Phys. Chem. A **105**, 10612 (2001).